

A New Oscillator for SI-Traceable Measurements in Atomic Force Microscopy

Gregory W. Vogl, Jason J. Gorman, Gordon A. Shaw, and Jon R. Pratt
 Manufacturing Engineering Laboratory
 National Institute of Standards and Technology (NIST), Gaithersburg, MD

Abstract

Atomic force microscopy (AFM) is used to image, measure, and manipulate surface atoms. In general, an atomic force microscope (see Fig. 1) consists of a microscale cantilever with a sharp tip at its end that is used to probe the sample surface. Forces between the tip and the sample lead to a cantilever deflection according to Hooke's law. Usually, manufacturers provide nominal cantilever stiffnesses (k) to AFM users, who then measure an approximate tip deflection (x) to estimate the tip-sample force ($F = kx$). Accordingly, AFM has been used to estimate small forces including van der Waals, chemical bonding, and Casimir forces¹.

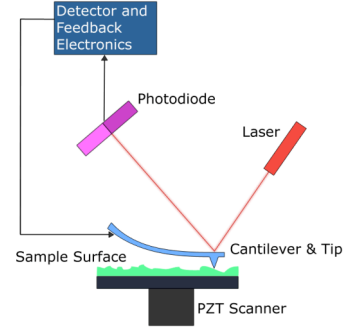


Figure 1. Block Diagram of an AFM.

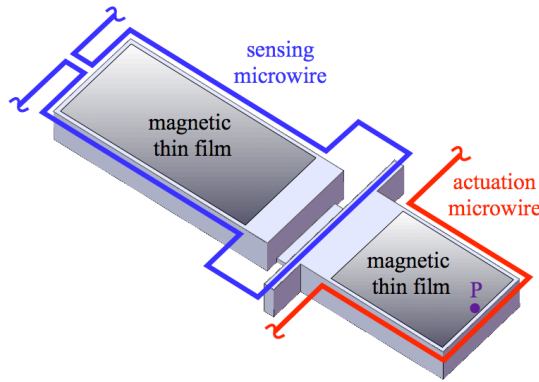


Figure 2. Micro-oscillator composed of a sensing side (left), an actuation side (right), and microwires.

forces² to measure SI-traceable nanonewton-level forces by standards of the National Institute of Standards and Technology (NIST).

However, commercial AFM suffers from a lack of accurate force measurements because there is presently no universal method to disseminate nanonewton-level forces that are *traceable* to the International System of Units (SI). In an attempt to solve this problem, a new micro-oscillator is being developed as a secondary standard for dissemination of SI-traceable nanonewton-level forces to AFM users. A novel analog control system will keep the actuation side of the device oscillating with a sinusoidal motion that is fairly insensitive to the quality factor, Q . Subsequently, point P in Fig. 2 will be calibrated as a velocity standard *ex situ*. Then, the device can be used *in situ* with applied electrostatic

The theoretical foundations, microfabrication steps, and preliminary experimental data for the device will be discussed in this presentation. First, we model the system as a two-degree-of-freedom system by treating the sensing and actuation masses as rigid bodies that rotate about one fixed axis, as seen in Figure 3. The rotational inertias of the sensing and actuation sides about the central axis are I_s and I_a , respectively. The torsional stiffness of the actuation side is κ_a , while the torsional stiffness of the sensing side is κ_s relative to the actuation side. Thus, the frequencies used for the model are ω_s and ω_a and are defined by $\omega_s^2 = \kappa_s / I_s$ and $\omega_a^2 = \kappa_a / I_a$, respectively.

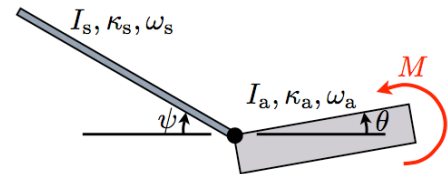


Figure 3. Approximate oscillator model.

Second, the device can be set up as a self-excited system for control purposes. Whenever the sensing side moves, a current is induced in the sensing microwire according to Faraday's law of magnetic induction.

This current is proportional to the angular velocity of the sensing side and can be amplified and fed through the actuation microwire. Accordingly, the magnetic field around the actuation microwire would induce a torque M on the magnetic thin film on the actuation side. This torque influences the motion of the actuation side and hence the sensing side through the flexural coupling.

Next, the gain on the sensing current is chosen so that the actuation side (e.g., point P in Fig. 2) settles to a sinusoidal limit cycle with a Q -insensitive amplitude. To achieve this goal, we created a nonlinear control system that transforms the self-excited system into a Rayleigh-like oscillator³. Hence, the control circuit that maintains the amplitude of the limit cycle for the actuation side will power the device. Also, the stability of the desired limit cycle is shown through use of Floquet theory⁴.

The control system works as expected, because the device could be calibrated in air (e.g., $Q = 10^2$) and then used in ultra-high vacuum (e.g., $Q = 10^4$) with a velocity shift within 0.4 percent. For example, as seen in Fig. 4(b), the actuation amplitude (the amplitude of θ) remains fairly constant as the quality factor changes by orders of magnitude. This happens because the control gain adapts itself to maintain the actuation amplitude. On the other hand, the sensing amplitude (the amplitude of ψ) in Fig. 4(a) increases significantly as the quality factor increases. We also note that the phase change of the actuation signal with Q is irrelevant, because the phase will not affect the velocity calibration.

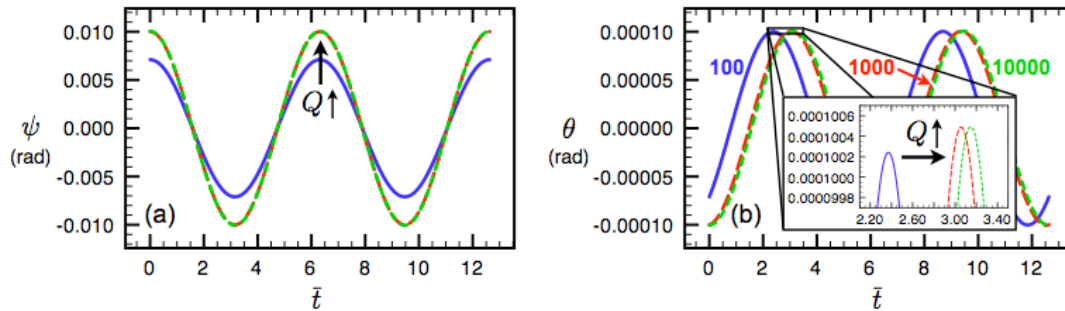


Figure 4. Typical limit cycles (angle vs. nondimensional time) for (a) ψ and (b) θ with $Q = 10^2, 10^3, \text{ or } 10^4$.

Finally, we examine the preliminary experimental data and also explain the possible future use of the new micro-oscillator as a stiffness sensor for high-speed AFM. As desired, the theoretical settling time of the control system is comparable to existing proportional-integral (PI) and proportional-integral-derivative (PID) methods for high-speed applications. However, because a stiffness change at point P in Fig. 2 does not cause a significant change in the system frequency, which is needed to sense the tip-surface distance for frequency-modulation AFM, another variable must be tracked for control purposes. Hence, we will discuss how a control signal for the device might be used instead of the system frequency to track stiffness changes.

¹e.g., G. L. Klimchitskaya *et al.*, Phys. Rev. A, **60**(5), pp. 3487–3494 (1999).

²e.g., P. J. Cumpson and J. Hedley, Nanotechnology, **14**, pp. 1279–1288 (2003).

³p. 147 of A. H. Nayfeh's *Introduction to Perturbation Techniques* (Wiley, 1981) describes the Rayleigh equation.

⁴pp. 158–172 of A. H. Nayfeh and B. Balachandran's *Applied Nonlinear Dynamics: Analytical, Computational, and Experimental Methods* (Wiley, 1995) describe Floquet theory.